EGU General Assembly 2020, May 4-8, 2020

Cooling effects on induced seismicity in supercritical geothermal systems

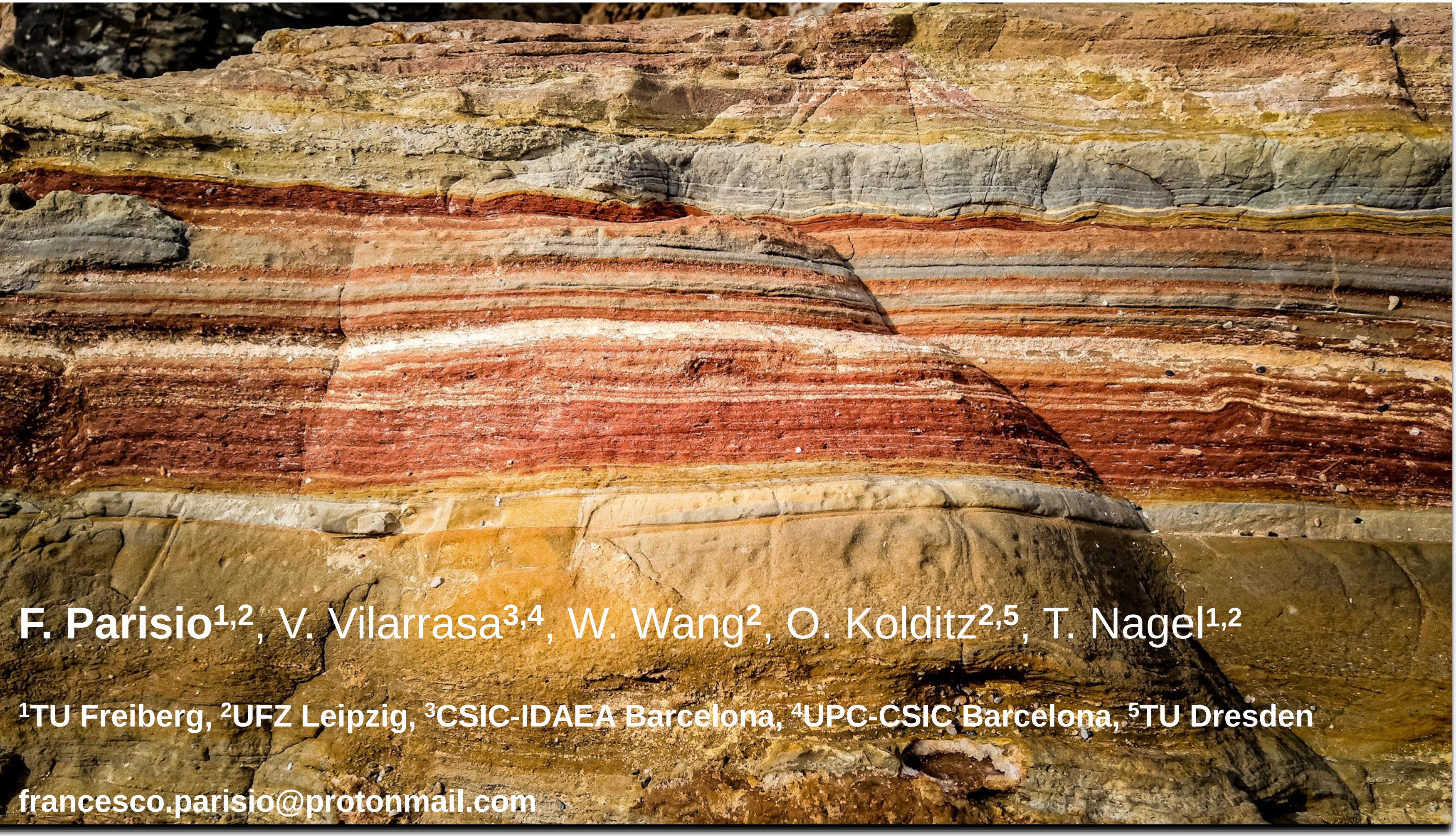

F. Parisio[1,2], V. Vilarrasa[3,4], W. Wang[2], O. Kolditz[2,5], T. Nagel[1,2]

[1]TU Freiberg, [2]UFZ Leipzig, [3]CSIC-IDAEA Barcelona, [4]UPC-CSIC Barcelona, [5]TU Dresden

francesco.parisio@protonmail.com

Cooling during re-injection affects mechanical stability

Thermal effects

Estimate of the re-injection temperature

Category	T_{min}	T_{max}	$< T >$	ΔT
	°C	°C	°C	°C
Hot Water	–	220	140	55
Low Enthalpy	220	250	235	131
Medium Enthalpy	250	300	275	186
High Enthalpy	250	330	290	169
Supercritical	–	–	457	322

Datum extrapolated for SC from Diaz et al. (2016)
Ren Sust Ener Rev

DT=300 ° C

Temperature and pressure changes affect stability

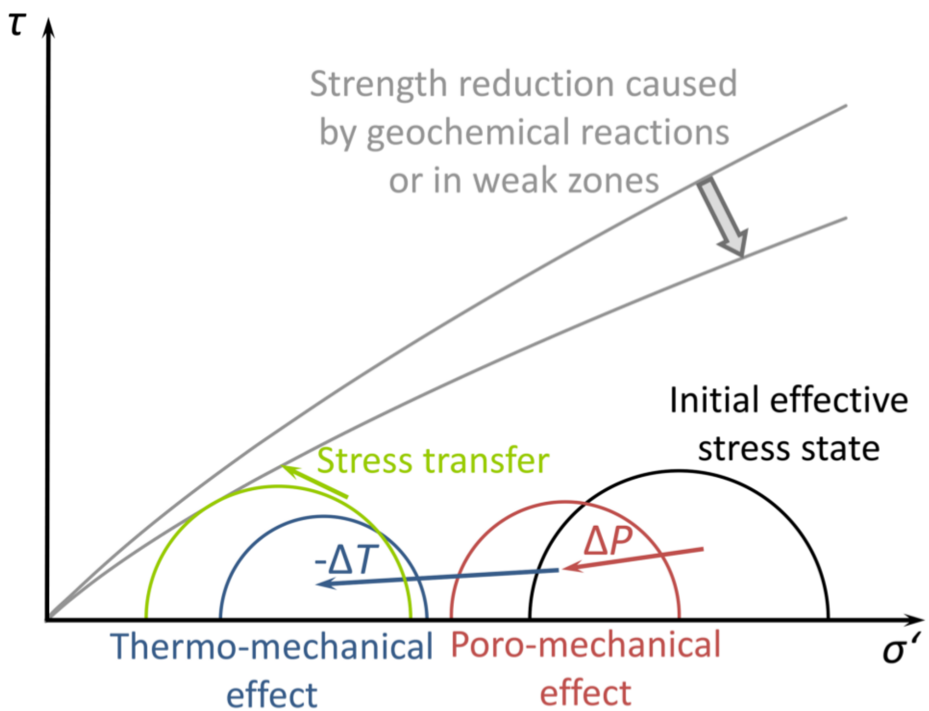

Vilarrasa et al. (2019) *Solid Earth*

Original study

Induced seismicity in supercritical geothermal systems

nature COMMUNICATIONS

ARTICLE

https://doi.org/10.1038/s41467-019-12146-0 OPEN

The risks of long-term re-injection in supercritical geothermal systems

Francesco Parisio[1,2*], Victor Vilarrasa[3,4], Wenqing Wang[1], Olaf Kolditz[2,5] & Thomas Nagel[1,2]

https://doi.org/10.1038/s41467-019-12146-0

Schematic model of ESGS doublet of production/injection

Conceptual model

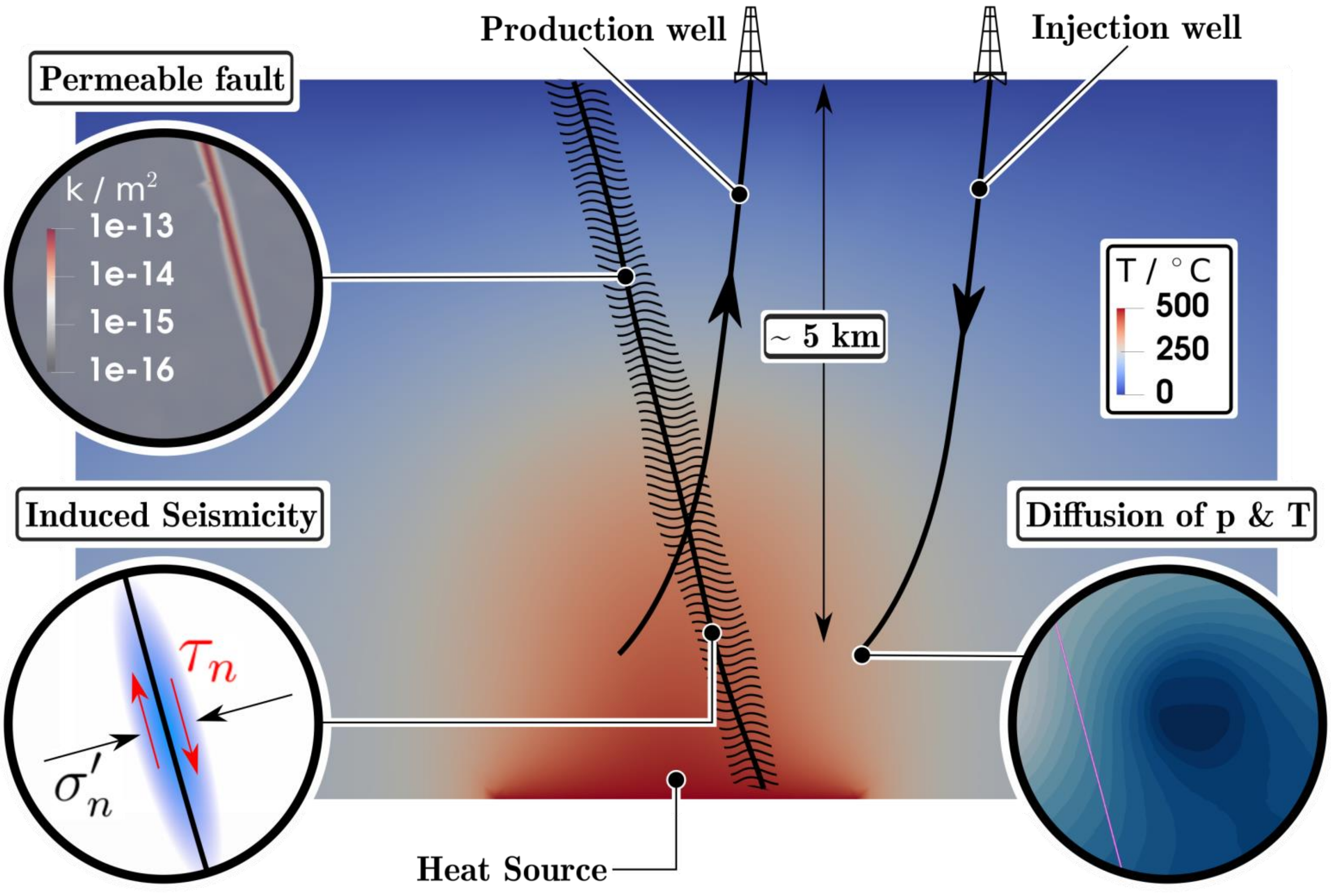

Reykjanes, ISL, January 2017

IDDP2:
4.5 km deep
~436 ° C

Fridhleifsson et al (2017) *Sci Drill*

Finite element model and permeability-porosity relationship

FEM model: IC and BC

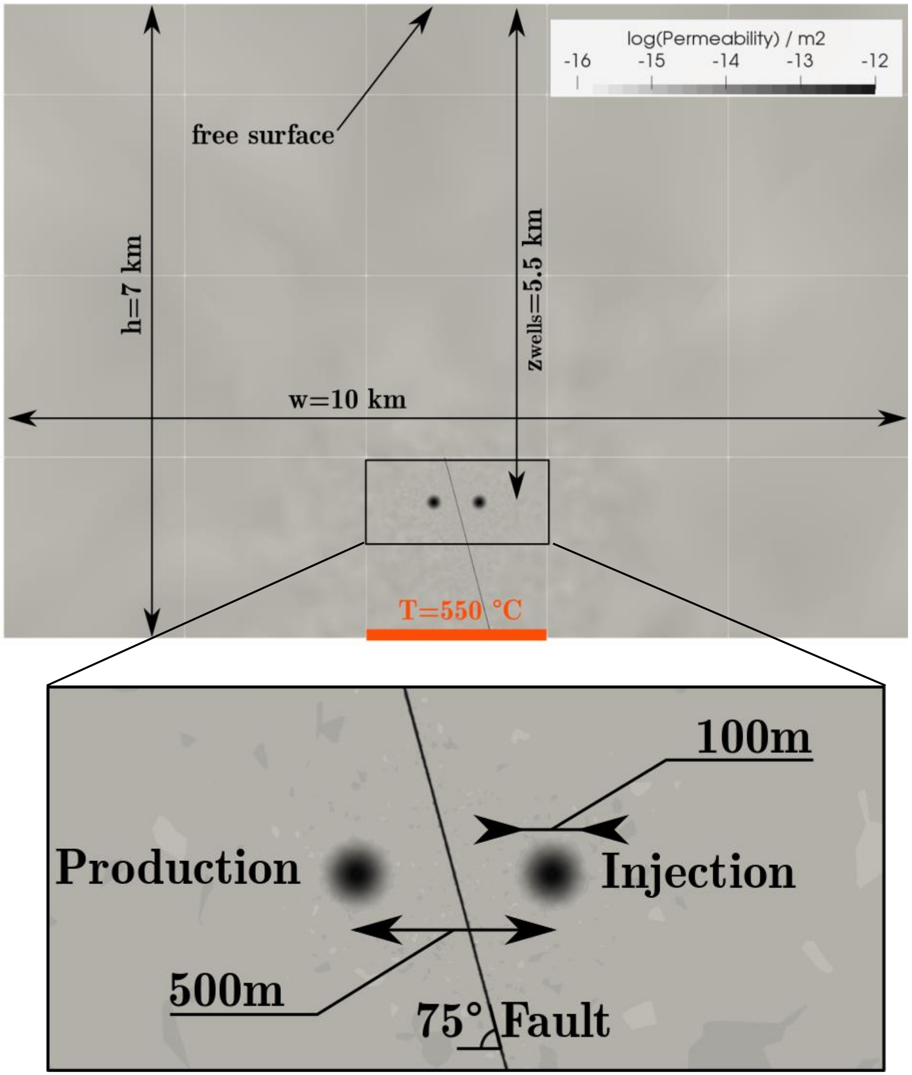

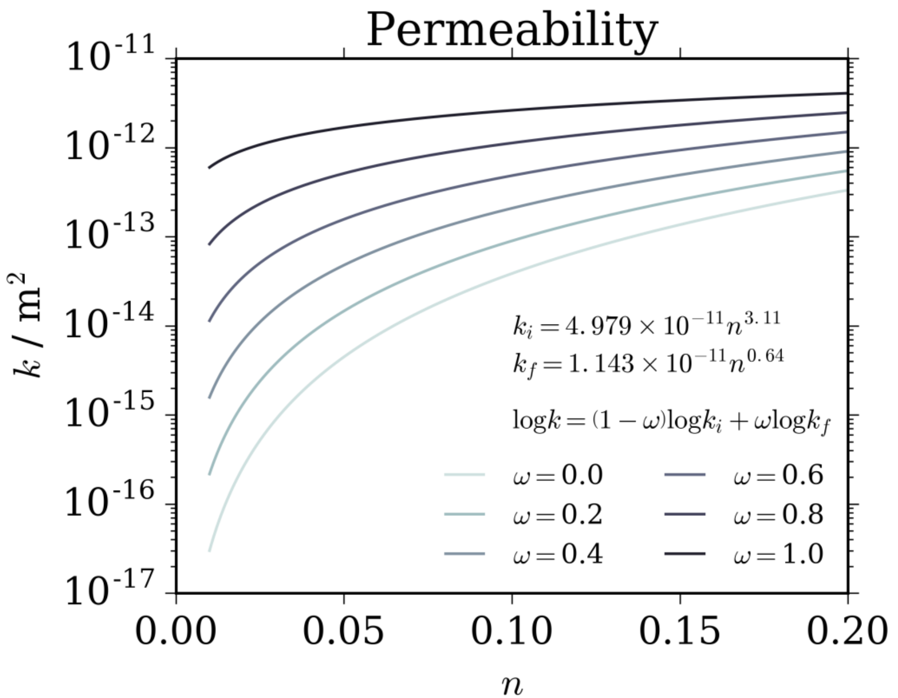

Lamur et al (2017) *Sci Rep*

Finite element model and permeability-porosity relationship

FEM model: IC and BC

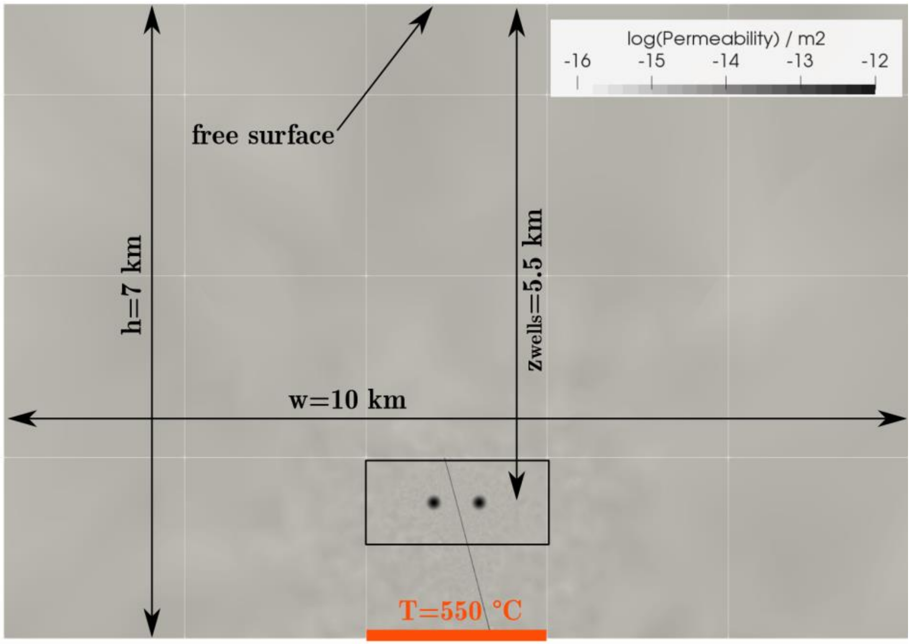

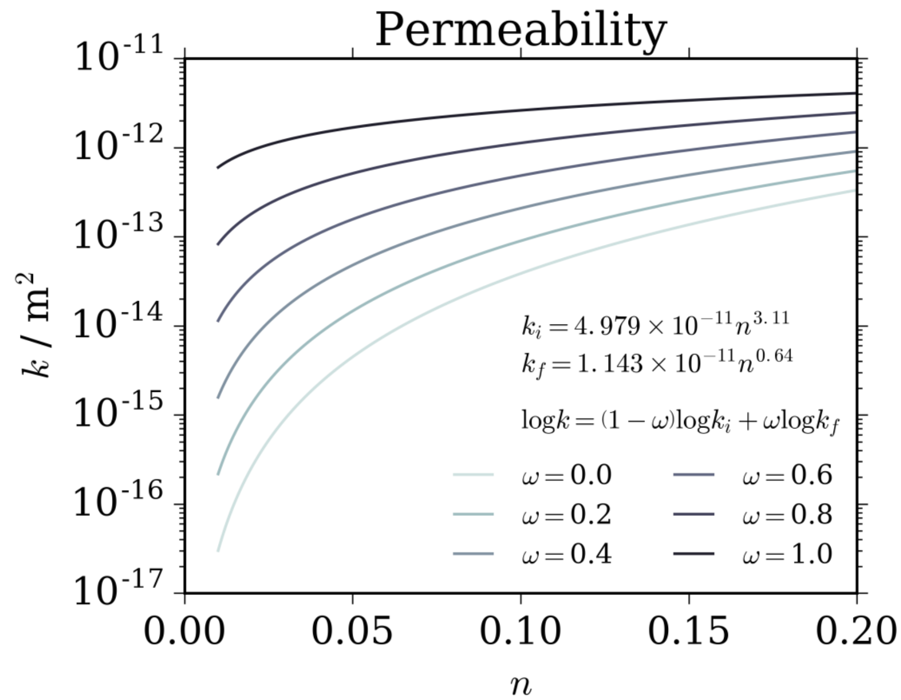

Lamur et al (2017) *Sci Rep*

Mass balance of solid skeleton

$$\frac{\mathrm{d_s} n}{\mathrm{d}t} = (1-n)\frac{1}{\rho_\mathrm{s}}\frac{\mathrm{d_s}\rho_\mathrm{s}}{\mathrm{d}t} + (1-n)\nabla\cdot\mathbf{v}_\mathrm{s} = (1-n)\left(\frac{1}{\rho_\mathrm{s}}\frac{\mathrm{d_s}\rho_\mathrm{s}}{\mathrm{d}t} + \dot{\epsilon}_\mathrm{v}\right)$$

$$\frac{1}{\rho_\mathrm{s}}\frac{\mathrm{d_s}\rho_\mathrm{s}}{\mathrm{d}t} = \frac{1}{1-n}\left[\frac{\alpha-n}{K_\mathrm{s}}\frac{\mathrm{d_s}p}{\mathrm{d}t} - 3\alpha_\mathrm{s}(\alpha-n)\frac{\mathrm{d_s}T}{\mathrm{d}t} - (1-\alpha)\frac{\mathrm{d_s}\epsilon_\mathrm{v}}{\mathrm{d}t}\right]$$

Porosity evolution

$$\frac{\mathrm{d_s} n}{\mathrm{d}t} = (\alpha-n)\left(\frac{1}{K_\mathrm{s}}\frac{\mathrm{d_s}p}{\mathrm{d}t} - 3\alpha_\mathrm{s}\frac{\mathrm{d_s}T}{\mathrm{d}t} + \frac{\mathrm{d_s}\epsilon_\mathrm{v}}{\mathrm{d}t}\right)$$

Finite element model and permeability-porosity relationship

FEM model: IC and BC

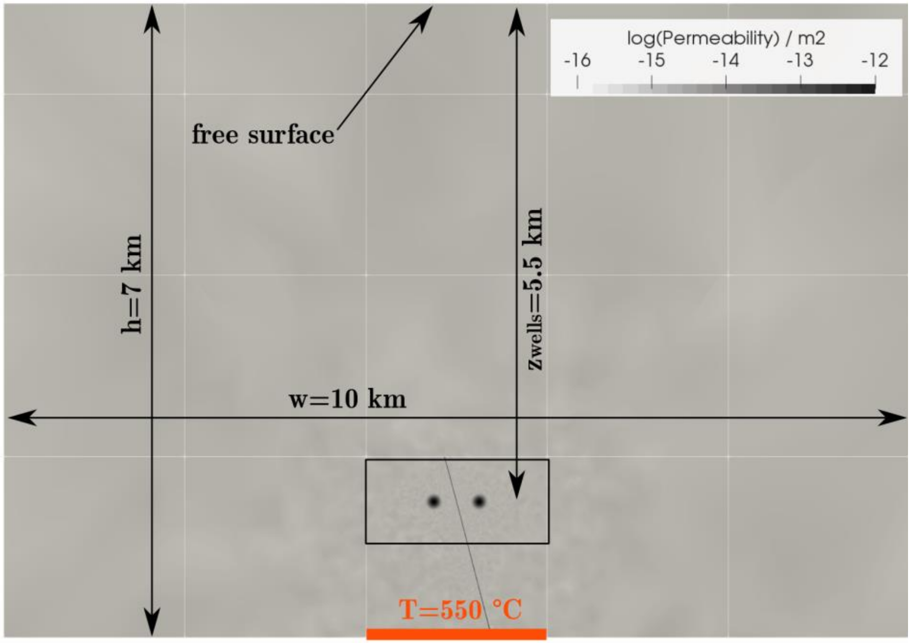

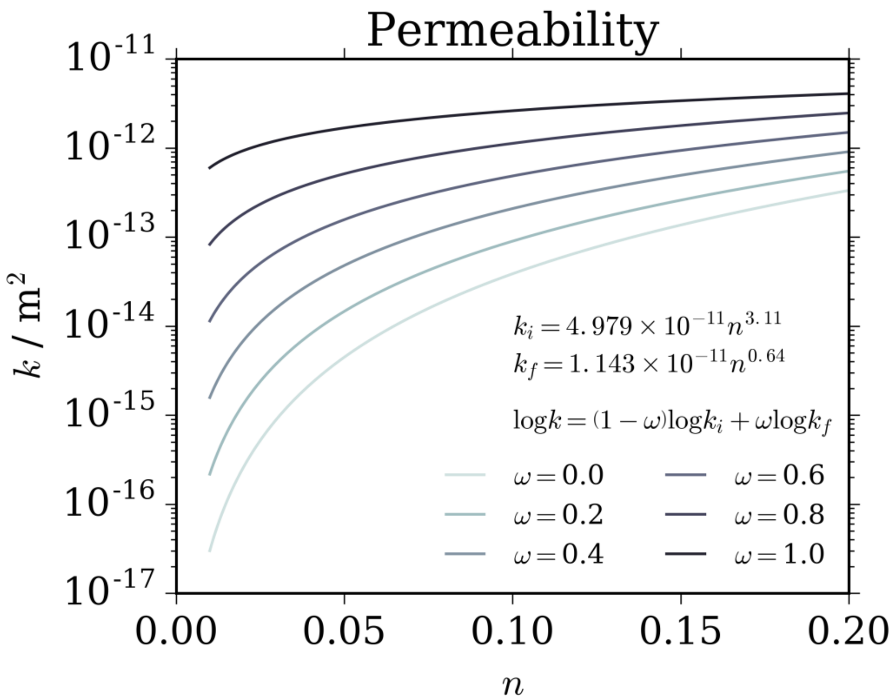

Lamur et al (2017) *Sci Rep*

Model parameters

Parameter	Rock mass	Fault	Units
n_0	0.01	0.05	-
ρ_s	2700	2700	kg m^{-3}
α_s	1×10^{-5}	1×10^{-5}	K^{-1}
c_s	950	950	J kg^{-1} K^{-1}
λ_s	3	3	W m^{-1} K^{-1}
E	60	20	GPa
ν	0.25	0.25	-
α	0.8	1.0	-
ϕ	30.0	30.0	°
σ_c	200.0	0.0	MPa

Porosity evolution

$$\frac{\mathrm{d_s}n}{\mathrm{d}t} = (\alpha - n)\left(\frac{1}{K_s}\frac{\mathrm{d_s}p}{\mathrm{d}t} - 3\alpha_s\frac{\mathrm{d_s}T}{\mathrm{d}t} + \frac{\mathrm{d_s}\epsilon_v}{\mathrm{d}t}\right)$$

Model equations for THM processes in porous media

System of partial differential equations

Energy conservation

$$(c\rho)_{\mathrm{m}} \frac{\mathrm{d_s}T}{\mathrm{d}t} - \nabla \cdot (\boldsymbol{\lambda}_{\mathrm{m}} \nabla T) + \rho_{\mathrm{w}} c_{\mathrm{w}} \mathbf{v} \cdot \nabla T = Q_{\mathrm{T}},$$

$$(c\rho)_{\mathrm{m}} = n\, \rho_{\mathrm{w}}\, c_{\mathrm{w}} + (1-n)\rho_{\mathrm{s}}\, c_{\mathrm{s}}$$

$$\boldsymbol{\lambda}_{\mathrm{m}} = n\lambda_{\mathrm{w}}\mathbf{I} + (1-n)\boldsymbol{\lambda}_{\mathrm{s}}$$

Specific heat and thermal conductivity of porous medium

Mass conservation

$$\left(n\beta_{\mathrm{w}} + \frac{\alpha - n}{K_{\mathrm{s}}}\right) \frac{\mathrm{d_s}p}{\mathrm{d}t} - \left[n\alpha_{\mathrm{w}} + 3\,(n-1)\,\alpha_{\mathrm{s}}\right] \frac{\mathrm{d_s}T}{\mathrm{d}t} + \nabla \cdot \mathbf{v} + \alpha \dot{\epsilon}_{\mathrm{v}} = Q_{\mathrm{H}}$$

$$\mathbf{v} = -\frac{\mathbf{k}}{\mu_{\mathrm{w}}} \left(\nabla p - \rho_{\mathrm{w}} \mathbf{g}\right)$$

Darcy‘s law

Momentum conservation

$$\frac{E}{2\,(1-2\nu)\,(1+\nu)} \nabla\left(\nabla \cdot \mathbf{u} - 3\alpha_{\mathrm{s}} \Delta T\right) + \frac{E}{(1-2\nu)} \nabla^2 \mathbf{u} - \nabla \cdot (\alpha p \mathbf{I}) + \left[n\rho_{\mathrm{w}} + (1-n)\rho_{\mathrm{s}}\right] \mathbf{g} = \mathbf{0}$$

$$\boldsymbol{\epsilon} = \frac{1}{2}\left[\nabla \mathbf{u} + (\nabla \mathbf{u})^{\mathrm{T}}\right]$$

Strain tensor

$$\alpha = 1 - \frac{K}{K_{\mathrm{s}}}$$

Biot‘s coefficient

Open source FEM solver: OpenGeoSys

Free, multi-platform software for the scientific modelling of coupled THMC processes in fractured porous media.

Available on GitHub https://github.com/ufz/ogs

Equations of state (EOS): IAPWS-IF97 on the free library **freesteam** http://freesteam.sourceforge.net/

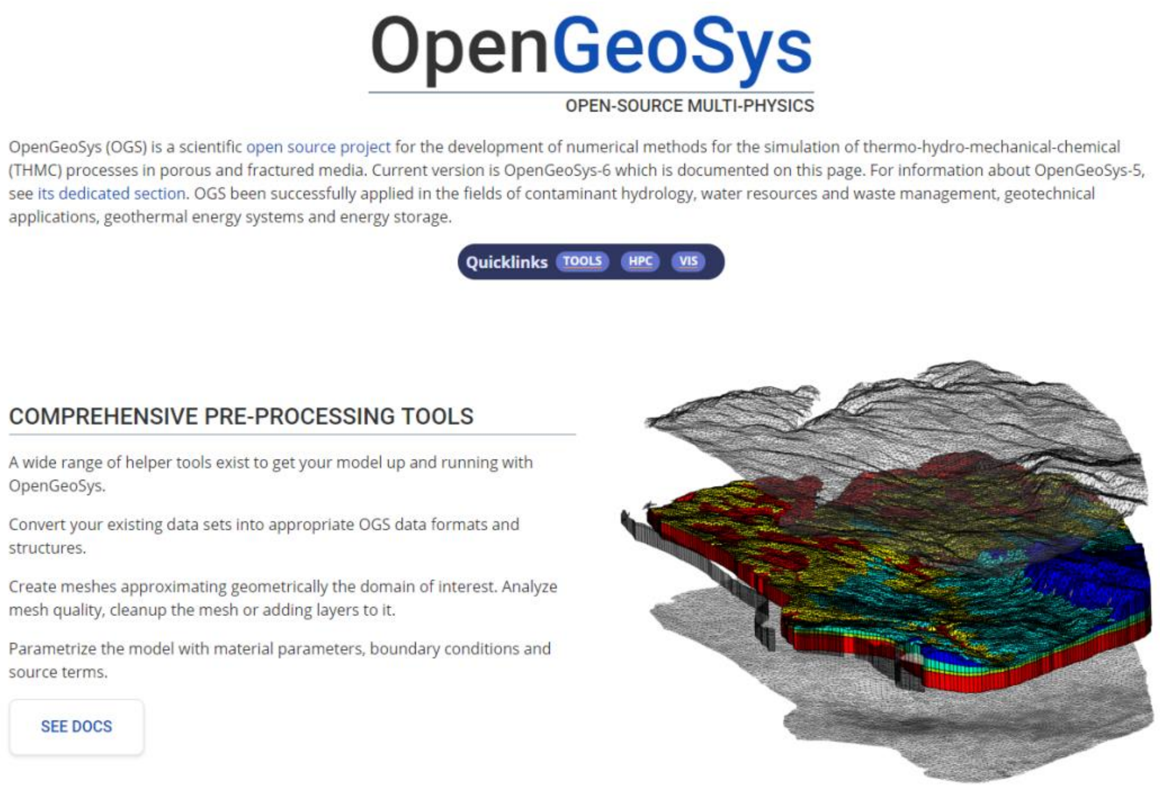

Density-driven flow forms convective cells in the reservoir

Initial conditions

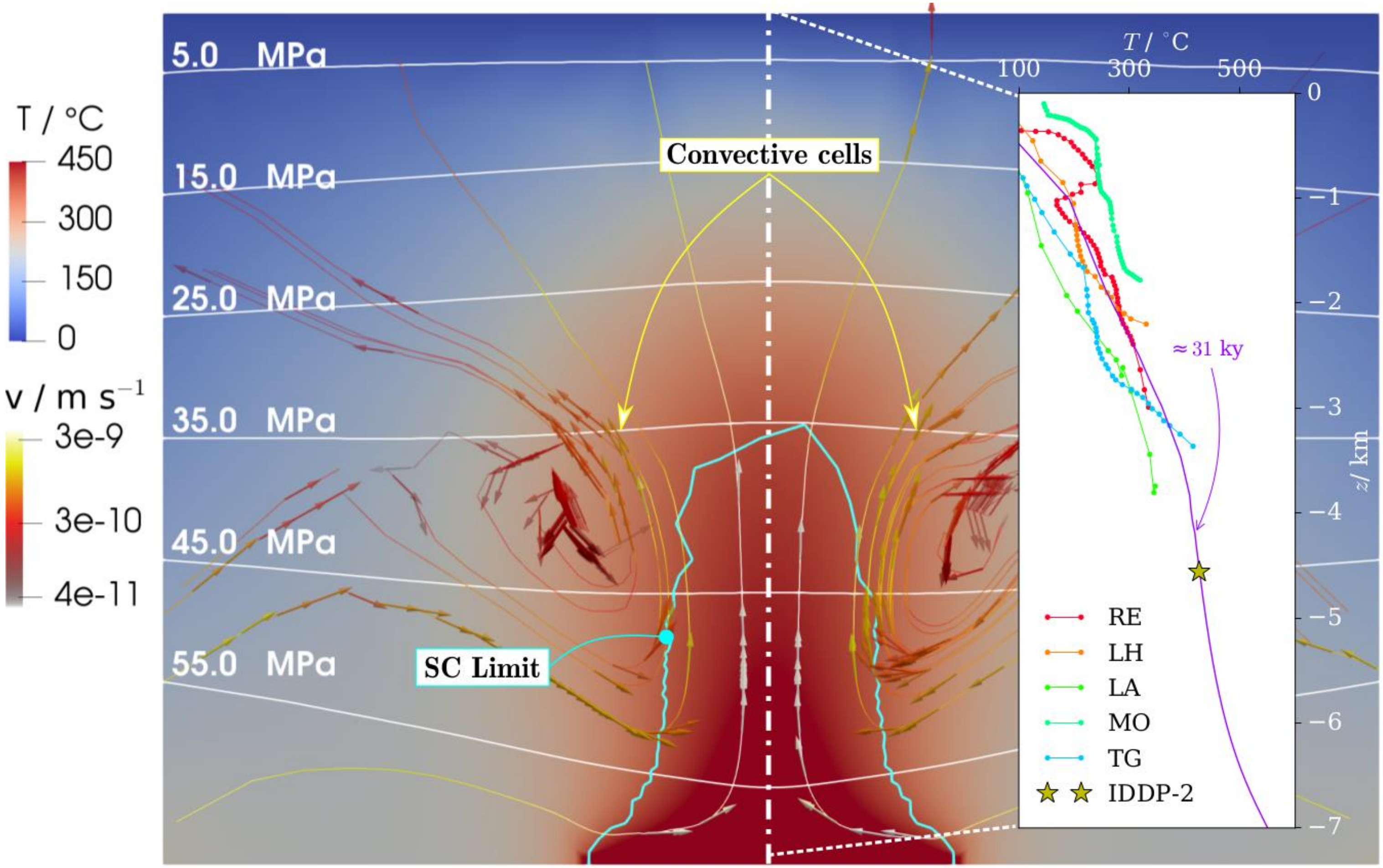

- RE: Reykjanes (ISL), Marks et al. (2015) *Chem Geol*, LH: Los Humeros (MEX), Luviano et al. (2015) *WGC*, LA: Larderello (ITA), Ebigbo et al. (2016) *Geoth Ener*, MO: Mofete (ITA), Carlino et al. (2016) *Ren Ener*, TG: The Geysers (USA), Garcia et al. (2016) *Geotherm*, IDDP2: Reykjanes (ISL), Fridhleifsson et al. (2017) *Sci Drill*

Pressure and temperature change follow different timescales

Geothermal doublet

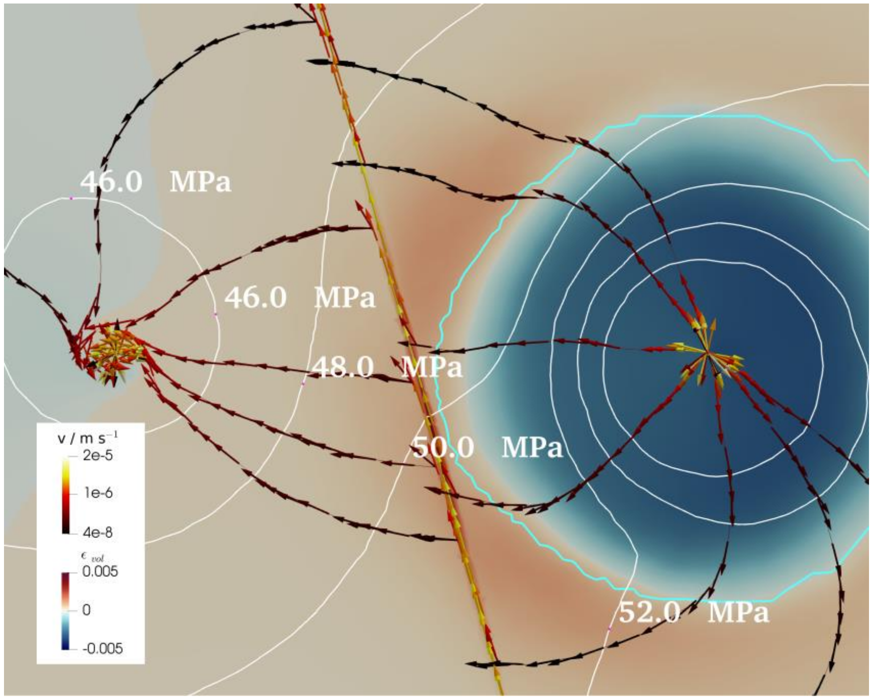

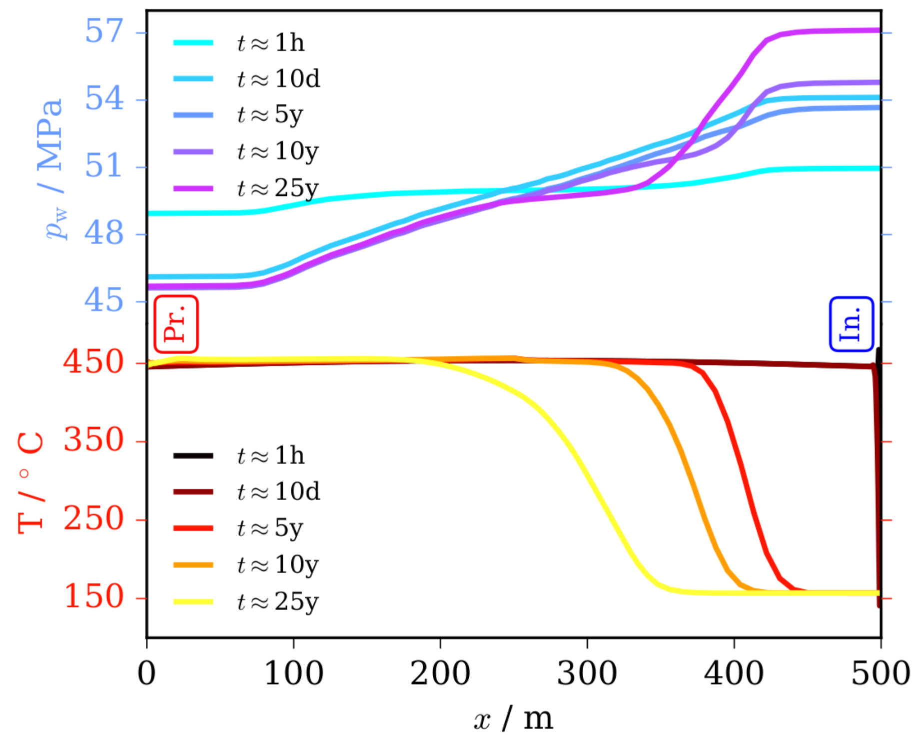

After 25 years of injection:

a. Liquid front has reached the fault

b. Quenched area contracts

c. Fault shows preferential flow paths

Thermal-advective process is slower than pore pressure diffusion

Cooling-induced stress controls fault stability

- Coulomb Failure Stress (CFS)

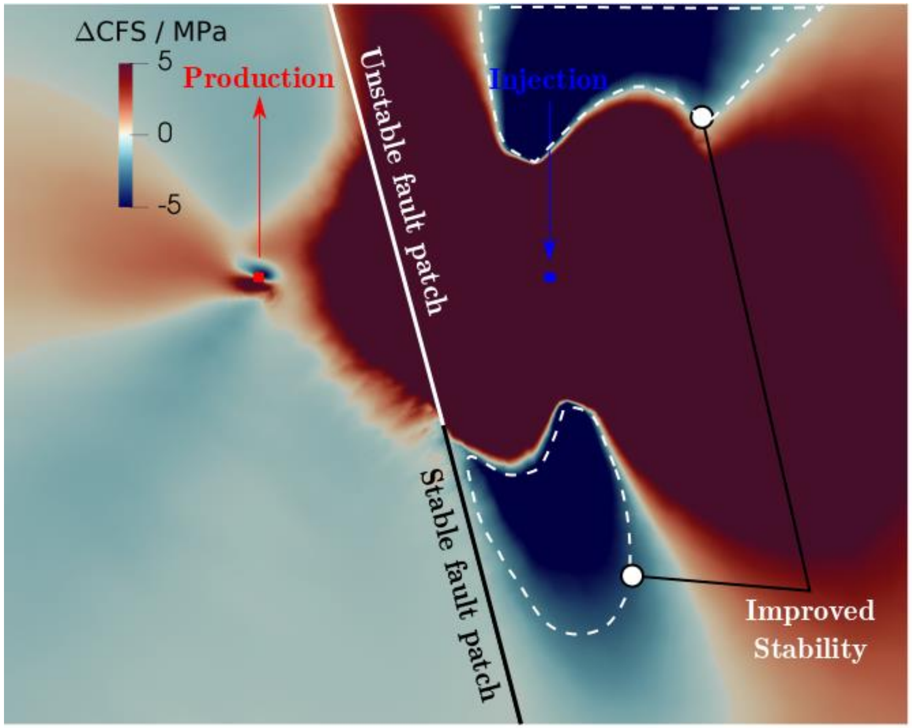

ΔCFS for cold water injection

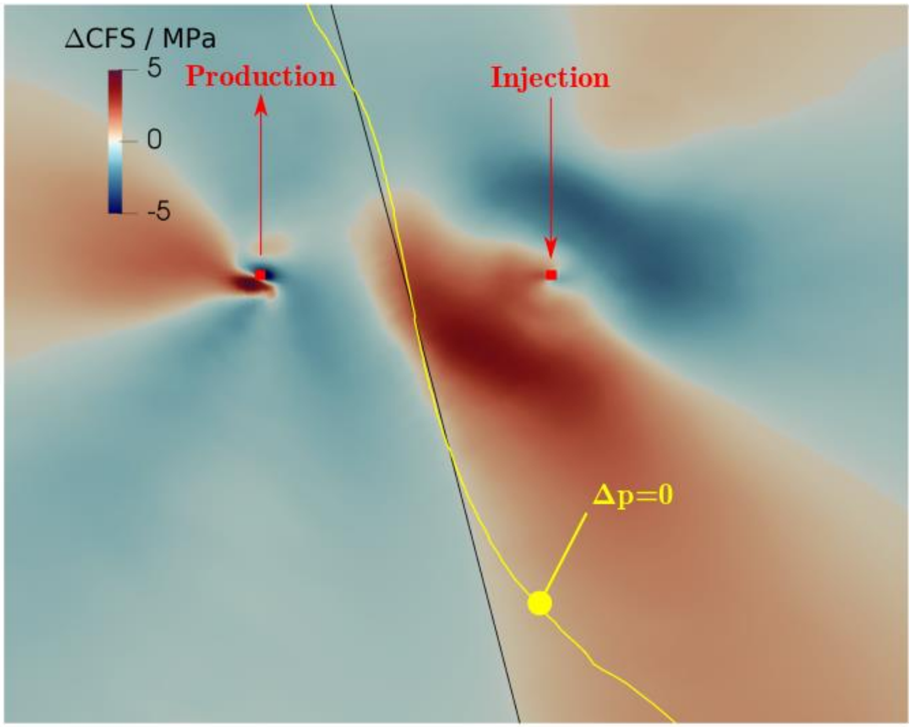

ΔCFS for isothermal injection

Where:

$$\mathrm{CFS} = \mid \tau_{\mathrm{n}} \mid + \mu \sigma'_{\mathrm{n}}$$

With:

$$\mu = 0.577$$

$$\boldsymbol{\sigma}' = \boldsymbol{\sigma} + \alpha p \mathbf{I}$$

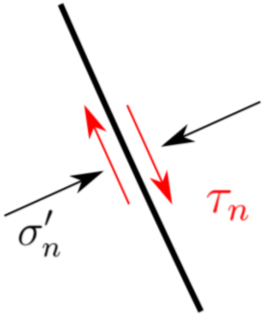

$\Delta\mathrm{CFS} > 0$ Increased instablity

Tensile failure can occur during cold water re-injection

Drucker-Prager failure

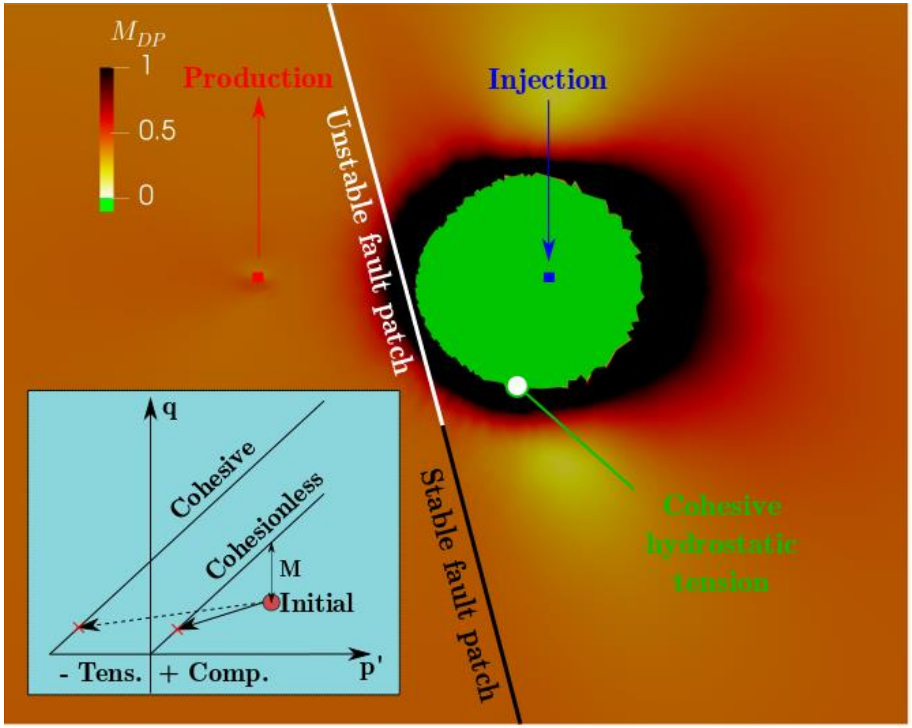

Drucker-Prager strenght for cold water injection

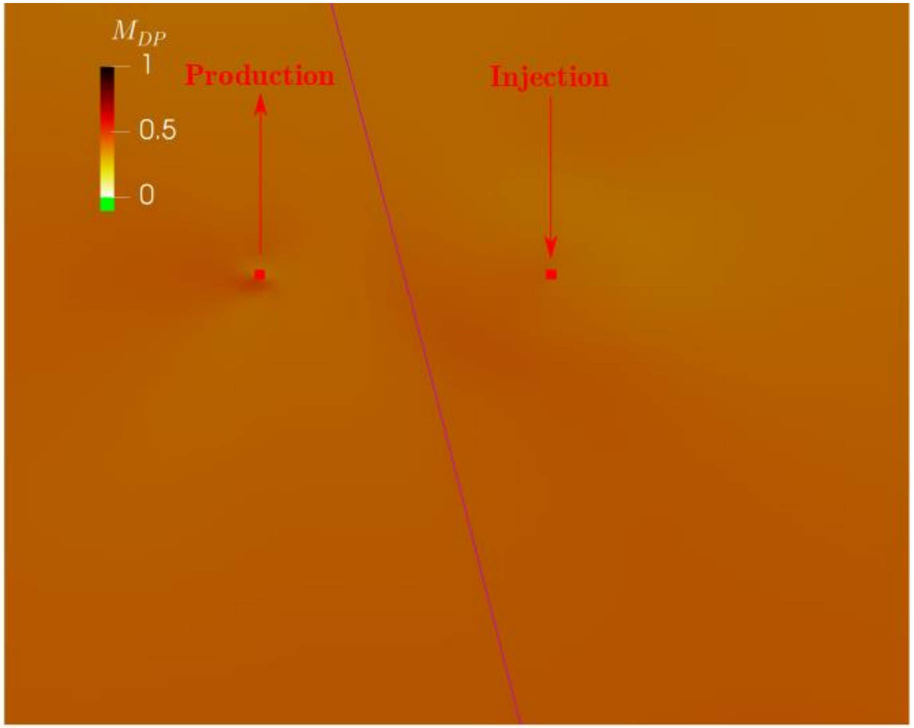

Drucker-Prager strenght for isothermal injection

Where:

$$q_{\text{dp}} = \frac{6\sin\phi}{3-\sin\phi}\left(-\sigma'_{\text{m}}\right) + \frac{6c'\cos\phi}{3-\sin\phi}$$

$$M_{\text{DP}} = q_{\text{dp}}/q$$

With:

$$\sigma'_{\text{m}} = \text{tr}\left(\boldsymbol{\sigma}'\right)/3$$

$$\boldsymbol{s} = \boldsymbol{\sigma}' - \mathbf{I}\sigma'_{\text{m}}$$

$$q = \sqrt{3\left(\boldsymbol{s}:\boldsymbol{s}\right)/2}$$

Seismicity is enhanced by cooling and delayed in the fault

Rate of seismic production

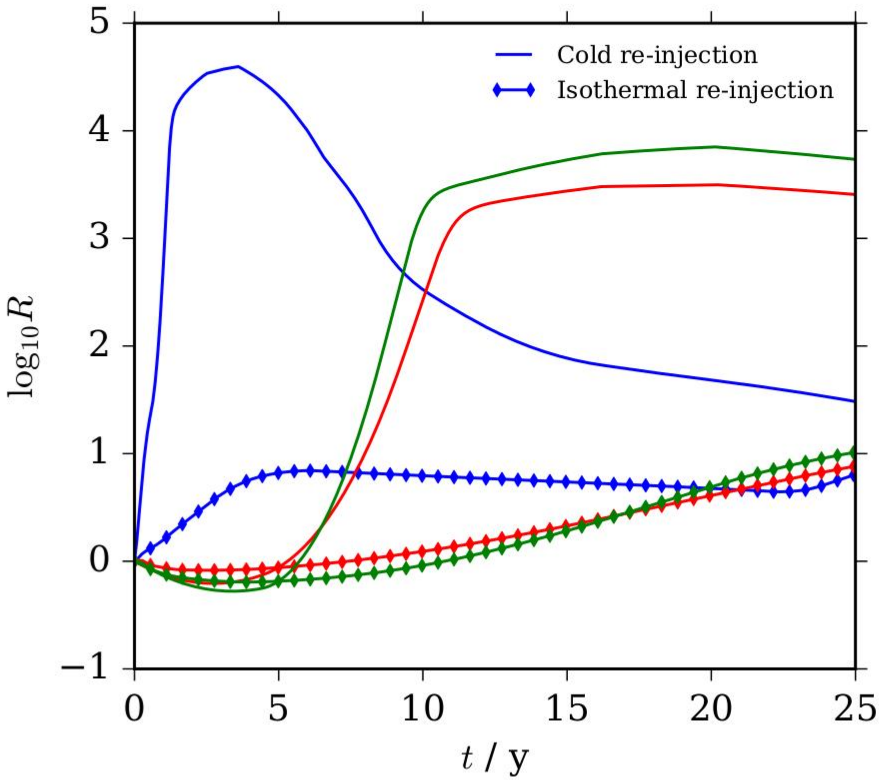

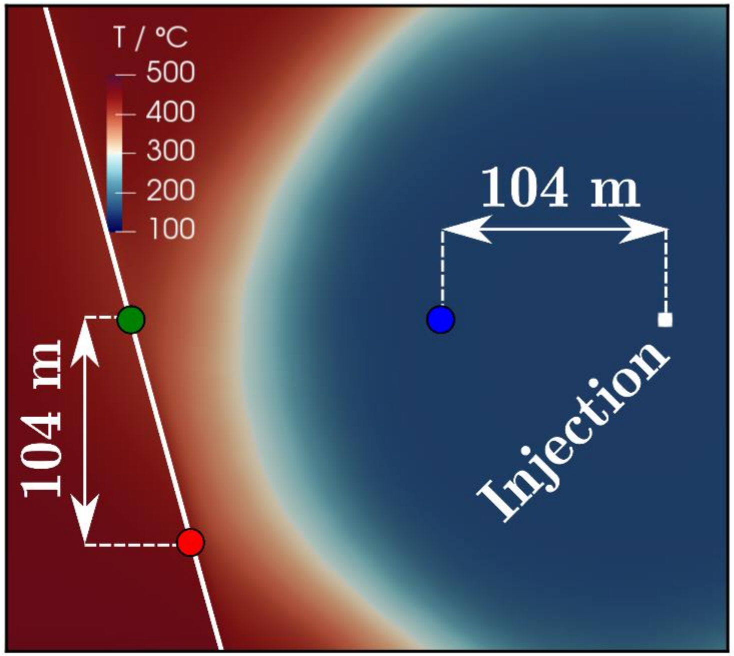

Where:

$$\dot{R} = R/t_a (\dot{\tau}_c/\dot{\tau}_0 - R)$$

With:

$$\dot{\tau}_0 = 1 \times 10^{-3}\,\text{MPa}\,\text{yr}^{-1}$$

$$\dot{\tau}_c = | \tau_n | + \mu \sigma'_n$$

$$t_a = A\sigma'_n/\dot{\tau}_0$$

Seagall and Lu (2015) *J Geoph Res*

The size of the mobilized fault patch is controlled by cooling

Fault-patch mobilization

$$\mu_{\mathrm{fr}} = \tau_{\mathrm{n}} / \left(-\sigma'_{\mathrm{n}}\right)$$

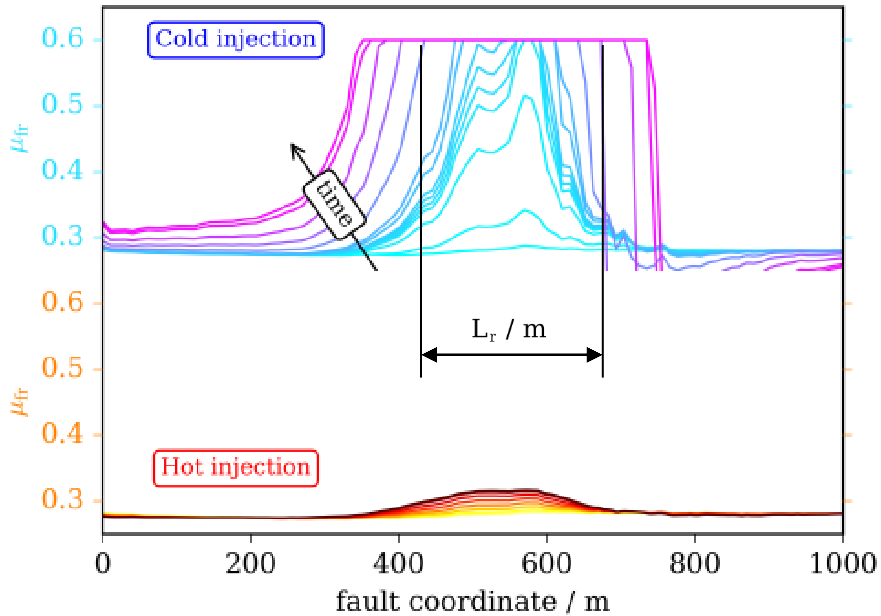

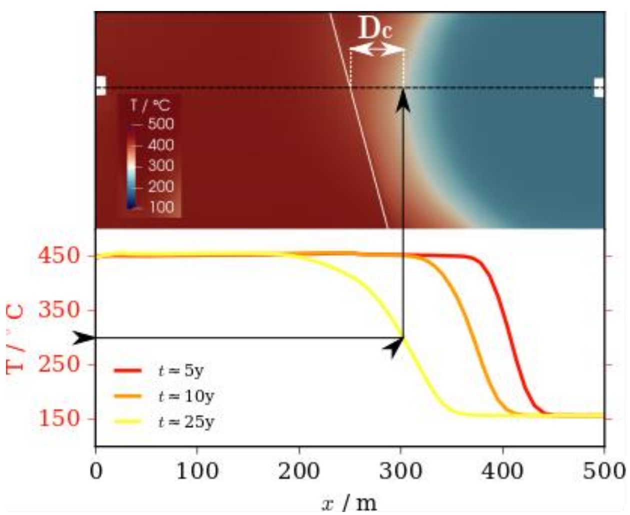

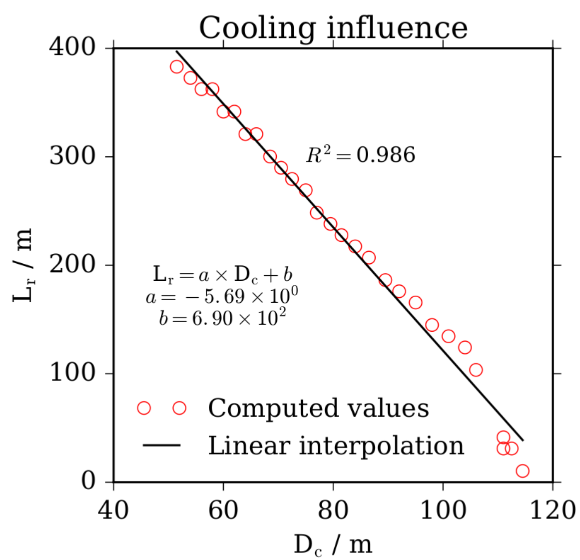

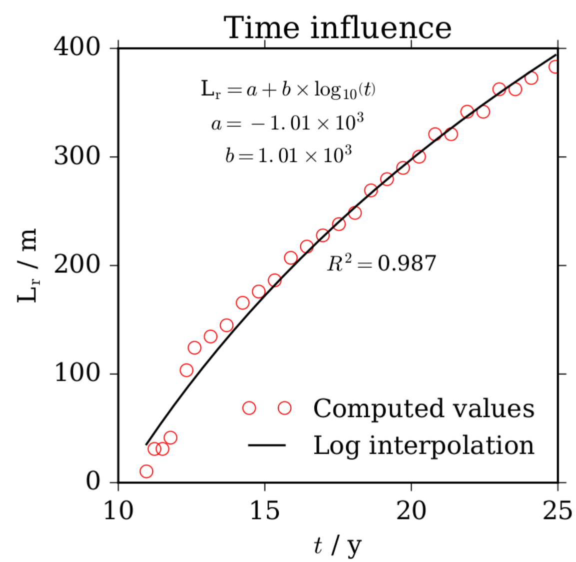

Conclusions, limitations and further research

Cooling controls seismicity in ESGS

Time in seismicity delay is due to advection

Fault location and re-injection temperature dominate the stability

Tensile fractures are likely to occur

Complex THM numerical analyses for reservoir management

ACKNOWLEDGEMENTS

This project has received funding from the European Union's Horizon 2020 research and innovation programme under grant agreement No. 727550

"The content of this presentation reflects only the authors' view. The Innovation and Networks Executive Agency (INEA) is not responsible for any use that may be made of the information it contains."

Contribution funded by the Deutsche Forschungsgemeinschaft (DFG, German Research Foundation) project number PA 3451/1-1